A&A 474, 385–392 (2007)
DOI: 10.1051/0004-6361:20077913

Astronomy & Astrophysics

Narrow-band surveys for very high redshift Lyman-α emitters

K. K. Nilsson[1,2], A. Orsi[3], C. G. Lacey[4], C. M. Baugh[4], and E. Thommes[5]

[1] Dark Cosmology Centre, Niels Bohr Institute, Copenhagen University, Juliane Maries Vej 30, 2100 Copenhagen, Denmark
e-mail: kim@dark-cosmology.dk
[2] European Southern Observatory, Karl-Schwarzschild-Straße 2, 85748 Garching bei München, Germany
[3] Department of Astronomy, Pontificia Universidad Católica, Casilla 306, Santiago 22, Chile
[4] Institute for Computational Cosmology, University of Durham, South Road, Durham DH1 3LE, UK
[5] Institut für Theoretische Physik, Universität Heidelberg, Philosophenweg 16, 69120 Heidelberg, Germany

Received 18 May 2007 / Accepted 30 August 2007

ABSTRACT

Context. Many current and future surveys aim to detect the highest redshift ($z \gtrsim 7$) sources through their Lyman-α (Lyα) emission, using the narrow-band imaging method. However, to date the surveys have only yielded non-detections and upper limits as no survey has reached the necessary combination of depth and area to detect these very young star forming galaxies.
Aims. We aim to calculate model luminosity functions and mock surveys of Lyα emitters at $z \gtrsim 7$ based on a variety of approaches calibrated and tested on observational data at lower redshifts.
Methods. We calculate model luminosity functions at different redshifts based on three different approaches: a semi-analytical model based on CDM, a simple phenomenological model, and an extrapolation of observed Schechter functions at lower redshifts. The results of the first two models are compared with observations made at redshifts $z \sim 5.7$ and $z \sim 6.5$, and they are then extrapolated to higher redshift.
Results. We present model luminosity functions for redshifts between $z = 7-12.5$ and give specific number predictions for future planned or possible narrow-band surveys for Lyα emitters. We also investigate what constraints future observations will be able to place on the Lyα luminosity function at very high redshift.
Conclusions. It should be possible to observe $z = 7-10$ Lyα emitters with present or near-future instruments if enough observing time is allocated. In particular, large area surveys such as ELVIS (Emission Line galaxies with VISTA Survey) will be useful in collecting a large sample. However, to get a large enough sample to constrain well the $z \geq 10$ Lyα luminosity function, instruments further in the future, such as an ELT, will be necessary.

Key words. cosmology: theory – cosmology: early Universe – galaxies: high-redshift – surveys

1. Introduction

One of the most promising ways of detecting very high redshift ($z \gtrsim 5$), star-forming galaxies is via narrow-band imaging surveys targeting Lyman-α (Lyα). In particular, redshifts $z \sim 5.7$ and 6.5 have been extensively surveyed by several groups (e.g. Ajiki et al. 2003; Hu et al. 2004; Shimasaku et al. 2005; Ouchi et al. 2005, 2007; Malhotra et al. 2005; Taniguchi et al. 2005; Tapken et al. 2006; Kashikawa et al. 2006). The current redshift record for a spectroscopically confirmed Lyα emitter (LEGO – Lyα Emitting Galaxy-building Object; see Møller & Fynbo 2001) is $z = 6.96$ (Iye et al. 2006) although Stark et al. (2007a) have suggested the discovery of two LEGOs at $z = 8.99$ and 9.32. The reason why narrow-band surveys are restricted to a discrete number of narrow redshift windows is the night sky OH emission lines. According to the OH line atlas of Rousselot et al. (2000), at Lyα redshifts $z_{\mathrm{Ly}\alpha} \gtrsim 7$ ($\lambda \gtrsim 9800$ Å) there are only a few possible wavelengths where a narrow-band filter can fit in between the OH sky lines. These correspond to $z_{\mathrm{Ly}\alpha} \approx 7.7$, 8.2, 8.8, 9.4 and 10.1–10.5. Several future surveys will target these windows in the sky aiming to detect very high redshift galaxies. Three narrow-band surveys for Lyα at redshift $z \sim 8.8$ have already been completed (Parkes et al. 1994; Willis & Courbin 2005; Cuby et al. 2007) but have only yielded upper limits. Future surveys planned for these redshifts include DaZle (Dark Ages Z Lyman-α Explorer, Horton et al. 2004) and ELVIS (Emission-Line galaxies with VISTA Survey, Nilsson et al. 2006b). Observations of very high redshift LEGOs have been proposed as an excellent probe of reionisation, through its effects on the Lyα emission line profile (e.g. Miralda-Escudé 1998; Miralda-Escudé & Rees 1998; Haiman 2002; Gnedin & Prada 2004), the luminosity function (e.g. Haiman & Cen 2005; Dijkstra et al. 2007a) and the clustering of sources (McQuinn et al. 2007).

We here focus on Lyα emission from star-forming galaxies, where the Lyα photons are emitted from gas which is photoionised by massive young stars. During recent years, theoretical work on Lyα emitting galaxies has made significant progress. There are three main aspects to these studies: *i*) predicting the numbers of star-forming galaxies as a function of star formation rate and redshift; *ii*) calculating the fraction of the Lyα photons which escape from galaxies into the IGM; and *iii*) calculating the factor by which the Lyα flux is attenuated by scattering in the IGM on its way to the observer. Accurate treatments of *ii*) and *iii*) are complicated because Lyα photons are resonantly scattered by hydrogen atoms, with the consequences that absorption of Lyα by dust in galaxies is hugely amplified, thereby reducing the escape fraction, and that even a small neutral fraction in the IGM can be effective at scattering Lyα photons out of the line-of-sight, thus attenuating the flux. Because of these

complications, most theoretical papers have chosen to concentrate on only one aspect, adopting simplified treatments of the other two aspects. Haiman & Spaans (1999) made predictions of the number counts of Lyα emitting galaxies by combining the Press-Schechter formalism with a treatment of the inhomogeneous dust distribution inside galaxies. Barton et al. (2004) and Furlanetto et al. (2005) calculated the numbers of Lyα emitters in cosmological hydrodynamical simulations of galaxy formation, but did not directly calculate the radiative transfer of Lyα photons. Radiative transfer calculations of the escape of Lyα photons from galaxies include those of Zheng & Miralda-Escudé (2002), Ahn (2004) and Verhamme et al. (2006) for idealised geometries, and Tasitsiomi (2006) and Laursen & Sommer-Larsen (2007) for galaxies in cosmological hydrodynamical simulations. The transmission of Lyα through the IGM has been investigated by Miralda-Escudé (1998), Haiman (2002), Santos (2004) and Dijkstra et al. (2007b), among others. Several authors (e.g. Haiman et al. 2000; Fardal et al. 2001; Furlanetto et al. 2005) have studied the effect of cold accretion to describe the nature of so-called Lyα blobs (Steidel et al. 2000; Matsuda et al. 2004; Nilsson et al. 2006a), see also Sect. 6.

Two models in particular, dissimilar in their physical assumptions, have been shown to be successful in reproducing the observed number counts and luminosity functions of Lyα emitting galaxies at high redshifts: firstly, the phenomenological model of Thommes & Meisenheimer (2005) which assumes that Lyα emitters are associated with the formation phase of galaxy spheroids, and secondly the semi-analytical model GALFORM (Cole et al. 2000; Baugh et al. 2005), which follows the growth of structures in a hierarchical, ΛCDM scenario. The GALFORM predictions for Lyα emitters are described in detail Le Delliou et al. (2005, 2006) and Orsi et al. (in prep.), who show that the model is successful in reproducing both the luminosity functions of Lyα emitting galaxies in the range $3 < z < 6$ and also their clustering properties.

In this paper we aim to provide model predictions to help guide the design of future planned or possible narrow-band surveys for very high redshift Lyα emitters. We make predictions based on three approaches: the semi-analytical and phenomenological models already mentioned, and an extrapolation from observations at lower redshift. In Sect. 2 we describe the different models used to make the predictions, and in Sect. 3 we present the predicted number counts and comparisons with observed luminosity functions at lower redshifts. In Sect. 4 we make number predictions for some specific future surveys. A brief discussion regarding what can be learned from these future surveys is found in Sect. 5. We give our conclusions in Sect. 6.

Throughout this paper, we assume a cosmology with $H_0 = 70\ \mathrm{km\,s^{-1}\ Mpc^{-1}}$, $\Omega_\mathrm{m} = 0.3$ and $\Omega_\Lambda = 0.7$, apart from the mock surveys discussed in Sect. 5, which use GALFORM models matched to the cosmology of the Millenium Run (Springel et al. 2005), (which has $H_0 = 73\ \mathrm{km\,s^{-1}\ Mpc^{-1}}$, $\Omega_\mathrm{m} = 0.25$ and $\Omega_\Lambda = 0.75$).

2. Models

We use three different approaches to predict the numbers of high redshift ($z > 7$) Lyα emitters. The models are based on very disparate assumptions. The first model is the semi-analytical model GALFORM (Le Delliou et al. 2005, 2006), the second is the phenomenological model of Thommes & Meisenheimer (2005), and the third model is based on directly extrapolating from observational data at lower redshifts.

Both the semi-analytical and phenomenological models assume that the fraction of Lyα photons escaping from galaxies is constant, and that the IGM is transparent to Lyα. The simple expectation is that before reionisation, the IGM will be highly opaque to Lyα, and after reionisation it will be mostly transparent. However, various effects can modify this simple behaviour; e.g. Santos (2004) finds that the transmitted fraction could be significant even before reionisation, while Dijkstra et al. (2007b) argue that attenuation could be important even after most of the IGM has been reionised. The WMAP 3-year data on the polarisation of the microwave background imply that reionisation occurred in the range $z \sim 8{-}15$ (Spergel et al. 2007), i.e. the IGM may be mostly transparent to Lyα at the redshifts of most interest in this paper. In any case, what is important for predicting fluxes of Lyα emitters is the product of the escape fraction from galaxies with the attenuation by the IGM. The two effects are in this respect degenerate.

2.1. Semi-analytical model

The semi-analytical model GALFORM (Cole et al. 2000; Baugh et al. 2005), which is based on ΛCDM, has been shown to be successful in reproducing a range of galaxy properties at both high and low redshift, including Lyα emitters in the range $z = 3{-}6$ (Le Delliou et al. 2005, 2006). A full description of GALFORM is given in these earlier papers, so we only give a brief summary here. GALFORM calculates the build-up of dark halos by merging, and the assembly of the baryonic mass of galaxies through both gas cooling in halos and galaxy mergers. It includes prescriptions for two modes of star formation – quiescent star formation in disks, and starbursts triggered by galaxy mergers – and also for feedback from supernovae and photoionisation. Finally, GALFORM includes chemical evolution of the gas and stars, and detailed stellar population synthesis to compute the stellar continuum luminosity from each galaxy consistent with its star formation history, IMF and metallicity (see Cole et al. 2000, for more details). The unextincted Lyα luminosity of each model galaxy is then computed from the ionising luminosity of its stellar continuum, assuming that all ionising photons are absorbed by neutral gas in the galaxy, with case B recombination.

The semi-analytical approach then allows us to obtain the properties of the Lyα emission of galaxies and their abundances as a function of redshift, calculating the star formation histories for the entire galaxy population, following a hierarchical evolution of the galaxy host haloes. In addition, when incorporated into an N-body simulation, we also obtain spatial clustering information. This model has been incorporated into the largest N-body simulation to date, the Millennium Simulation (Springel et al. 2005), to predict clustering properties of Lyα galaxies. These results will be presented in a forthcoming paper (Orsi et al., in prep.).

The version of GALFORM which we use here is the one described in Baugh et al. (2005) and Le Delliou et al. (2006), with the same values for parameters. The parameters in the model were chosen in order to match a range of properties of present-day galaxies, as well as the numbers of Lyman Break and sub-mm galaxies at $z \sim 2{-}3$. We assume a Kennicutt IMF for quiescent star formation, but a top-heavy IMF for starbursts, in order to reproduce the numbers of sub-mm galaxies. The only parameter which has been adjusted to match observations of Lyα emitters is the Lyα escape fraction, which is taken to have a constant value $f_\mathrm{esc} = 0.02$, regardless of galaxy dust properties. Le Delliou et al. (2006) show that the simple choice of a

constant escape fraction $f_{\rm esc} = 0.02$ predicts luminosity functions of Lyα emitters in remarkably good agreement with observational data at $3 < z < 6$. Le Delliou et al. (2006) also compared the predicted Lyα equivalent widths with observational data at $3 < z < 5$, including some model galaxies with rest-frame equivalent widths of several 100 Å, and found broad consistency. For this reason, we use the same value $f_{\rm esc} = 0.02$ for making most of our predictions at $z > 7$. However, since the value of the escape fraction at $z > 7$ is a priori uncertain in the models (e.g. it might increase with redshift if high redshift galaxies are less dusty) we also present some predictions for other values of $f_{\rm esc}$.

Reionisation of the IGM affects predictions for the numbers of Lyα emitters in deep surveys in two ways: *i*) feedback from photo-ionisation inhibits galaxy formation in low-mass halos; and *ii*) reionisation changes the opacity of the IGM to Lyα photons travelling to us from a distant galaxy, as discussed above. GALFORM models the first effect in a simple way, approximating reionisation as being instantaneous at redshift $z_{\rm reion}$ (see Le Delliou et al. 2006, for more details). We assume $z_{\rm reion} = 10$, in line with the WMAP 3-year results (Spergel et al. 2007). As was shown in Le Delliou et al. (2006; see their Fig. 8), as far as the feedback effect is concerned, varying $z_{\rm reion}$ over the range $7 \lesssim z_{\rm reion} \lesssim 10$ does not have much effect on the bright end of the Lyα luminosity function most relevant to current and planned surveys. For example, varying $z_{\rm reion}$ between 7 and 10 changes the predicted luminosity function at $L_{{\rm Ly}\alpha} > 10^{41.5}$ erg s^{-1} by less than 10% for $z \sim 7$–10.

2.2. Phenomenological model

The phenomenological model of Thommes & Meisenheimer (2005; TM05 hereafter) assumes that the Lyα emitters seen at high redshift are galaxy spheroids seen during their formation phase. We summarise the main features here, and refer the reader to TM05 for more details. The model is normalised to give the observed mass function of spheroids at $z = 0$, which is combined with a phenomenological function that gives the distribution of spheroid formation events in mass and redshift. Each galaxy is assumed to be visible as a Lyα emitter during an initial starburst phase of fixed duration (and Gaussian in time), during which the peak SFR is proportional to the baryonic mass and inversely proportional to the halo collapse time. The effects of the IMF and the escape fraction on the Lyα luminosity of a galaxy are combined into a single constant factor (i.e. the escape fraction is effectively assumed to be constant). With these assumptions, the luminosity function of Lyα emitters can be computed as a function of redshift. The free parameters in the model were chosen by TM05 to match the observed number counts of Lyα emitters at $3.5 < z < 5.7$ (analogously to the choice of $f_{\rm esc}$ in the GALFORM model). This model does not include any effects from reionisation.

2.3. Observational extrapolation

Our third approach is to assume that the Lyα luminosity function is a Schechter function at all redshifts, following

$$\phi(L){\rm d}L = \phi^\star (L/L^\star)^\alpha \exp(-L/L^\star){\rm d}L/L^\star \quad (1)$$

and to derive the Schechter parameters α, $\phi^\star$ and $L^\star$ at high redshifts by extrapolating from the observed values at lower redshifts. For our extrapolation, we use fits to observations at redshift $z \approx 3$ (van Breukelen et al. 2005; Gronwall et al. 2007; Ouchi et al. 2007), $z = 3.7$ (Ouchi et al. 2007), $z = 4.5$ (Dawson et al. 2007), $z \approx 5.7$ (Malhotra & Rhoads 2004; Shimasaku et al. 2006; Ouchi et al. 2007) and $z \approx 6.5$ (Malhotra & Rhoads 2004; Kashikawa et al. 2006), as found in Table 1. We make linear fits to $\log\phi^\star$ and $\log L^\star$ vs. z, and extrapolate to higher redshift. For simplicity, we assume a fixed faint end slope of $\alpha = -1.5$. We do not make any corrections for any possible effects of reionisation or IGM opacity. The extrapolated values are given in Table 2.

Table 1. Parameters of the fitted Schechter function in previously published papers. References are 1) van Breukelen et al. (2005), 2) Gronwall et al. (2007), 3) Ouchi et al. (2007), 4) Dawson et al. (2007), 5) Malhotra & Rhoads (2004), 6) Shimasaku et al. (2006), and 7) Kashikawa et al. (2006). References 3–6 fit for three faint end slopes ($\alpha = -1.0, -1.5$ and -2.0), but here we only reproduce the results for fits with $\alpha = -1.5$ as we fix the slope in our calculations. Malhotra & Rhoads (2004) do not give error bars on the fits. Dawson et al. (2007) fix the slope to $\alpha = -1.6$.

Ref.	Redshift	α	$\log\phi^\star{\rm Mpc}^{-3}$	$\log L^\star$erg/s
1	∼3.2	−1.6	$-2.92^{+0.15}_{-0.23}$	$42.70^{+0.13}_{-0.19}$
2	3.1	$-1.49^{+0.45}_{-0.54}$	−2.84	$42.46^{+0.26}_{-0.15}$
3	3.1	−1.5	$-3.04^{+0.10}_{-0.11}$	$42.76^{+0.06}_{-0.06}$
3	3.7	−1.5	$-3.47^{+0.11}_{-0.13}$	$43.01^{+0.07}_{-0.07}$
4	4.5	−1.6	$-3.77^{+0.05}_{-0.05}$	$43.04^{+0.14}_{-0.14}$
5	5.7	−1.5	−4.0	43.0
6	5.7	−1.5	$-3.44^{+0.20}_{-0.16}$	$43.04^{+0.12}_{-0.14}$
3	5.7	−1.5	$-3.11^{+0.29}_{-0.31}$	$42.83^{+0.16}_{-0.16}$
5	6.5	−1.5	−3.3	42.6
7	6.5	−1.5	$-2.88^{+0.24}_{-0.26}$	$42.60^{+0.12}_{-0.10}$

Table 2. Extrapolated parameters of the observed Schechter function at higher redshifts. The faint end slope is fixed to $\alpha = -1.5$.

Redshift	$\log\phi^\star$ Mpc^{-3}	$\log L^\star$ erg/s
7.7	−3.73 ± 0.50	42.88 ± 0.24
8.2	−3.80 ± 0.50	42.89 ± 0.24
8.8	−3.88 ± 0.50	42.91 ± 0.24
9.4	−3.96 ± 0.50	42.92 ± 0.24
12.5	−4.38 ± 0.50	42.99 ± 0.24

3. Luminosity functions

The possible Lyα redshifts between $z = 7$ and $z = 10$ where a narrow-band filter can be placed are $z_{{\rm Ly}\alpha} = 7.7, 8.2, 8.8$, and 9.4. Redshifts beyond 10 are unreachable with ground-based instruments of the near-future. However, one possibility for $z > 10$ surveys may be the James Webb Space Telescope (JWST, see Sect. 4.3) and so we also make predictions for redshift $z_{{\rm Ly}\alpha} = 12.5$.

First, we compare the Lyα luminosity functions predicted by the semi-analytical (GALFORM) and phenomenological (TM05) models with current observational data at $z \sim 6$. This comparison is shown in Fig. 1, where we compare the models with the cumulative luminosity functions measured in several published surveys at $z = 5.7$ and $z = 6.5$. We can see that both models match the observational data reasonably well, once one takes account of the observational uncertainties. The error bars on the observational data points, omitted in the plot in order to not confuse the points, are large, at the bright end of the luminosity function due to small number statistics, and at the faint end due to incompleteness in the samples. The shallow slopes at the faint ends of the Taniguchi et al. (2005) and Ouchi et al. (2007)

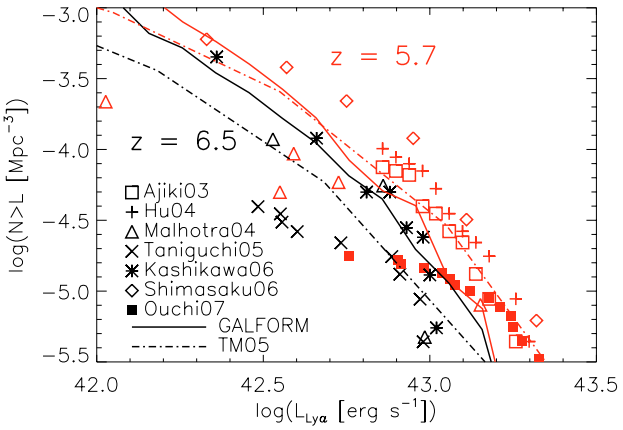

Fig. 1. Plot of luminosity functions at redshifts $z = 5.7$ and 6.5. Red points and lines are at redshift $z = 5.7$, black points/lines at redshift $z = 6.5$. Points are observations by Ajiki et al. (2003; redshift 5.7, squares), Hu et al. (2004; redshift 5.7, pluses), Taniguchi et al. (2005; redshift 6.5, crosses), Shimasaku et al. (2006; redshift 5.7, diamonds), Kashikawa et al. (2006; redshift 6.5, stars), Malhotra & Rhoads (2004; redshift 5.7 and 6.5, triangles) and Ouchi et al. (2007; redshift 5.7, filled squares). Solid lines show the GALFORM model (with escape fraction $f_{\rm esc} = 0.02$), dot-dashed lines the TM05 model. Note that the Taniguchi et al. (2005) and the Ouchi et al. (2007) samples are the spectroscopic samples only.

luminosity functions may be due to spectroscopic incompleteness. Both models fit the observations well. Hence we conclude that both of these models can be used to extrapolate to higher redshifts.

We now have three methods of extrapolating to higher redshifts, when the direct extrapolation of the Schechter function from lower redshifts is included. In Fig. 2 we plot the predicted luminosity functions at $z = 7.7$, 8.8 and 12.5 computed by these three methods. For other redshifts, the curves may be interpolated. For GALFORM, we show predictions for the standard value of the escape fraction $f_{\rm esc} = 0.02$ in the left panel, and for a larger value $f_{\rm esc} = 0.2$ in the right panel. This illustrates the sensitivity of the predictions to the assumed value of $f_{\rm esc}$ at high redshift. The predictions from the other two models are plotted identically in both panels, since they do not explicitly include the escape fraction as a parameter. GALFORM predictions for the numbers of Lyα emitters at $z > 7$ were also given in Le Delliou et al. (2006). We can see that the predictions from the different methods are fairly similar at $z = 7.7$, but gradually diverge from each other with increasing redshift. For the highest redshift, $z = 12.5$, the TM05 model fails in producing a prediction due to numerical problems. We note that making predictions for $z = 12.5$ is challenging, for several reasons. Even though only ∼200 Myr separate the ages of the Universe between redshift 8.8 and 12.5, the Universe went through an important transition at this time as reionisation occurred (Spergel et al. 2007). However, we do not know exactly how and when this happened. Also, during this epoch the structure in the dark matter (and hence also in galaxies) was building up very rapidly. This underlines the interest of obtaining observational constraints at these redshifts.

The hatched regions in Fig. 2 show the region of the luminosity function diagram that has been observationally excluded at $z = 8.8$ by Willis & Courbin (2005) and Cuby et al. (2006). The former survey was deeper but in a smaller area, whereas the latter was more shallow over a larger area, hence the two-step appearance of the hatched area. From the plot, it is obvious that their non-detections are perfectly consistent with our theoretical models, although the GALFORM model with the non-standard escape fraction $f_{\rm esc} = 0.2$ is marginally excluded.

4. Future surveys

In this section, we discuss more specific predictions for several planned and possible future surveys. For all calculations, we assume a simple selection on the flux of the Lyα emission line, with no additional selection on the equivalent width (i.e. we include all galaxies with $EW_{\rm Ly\alpha} \geq 0$). We also assume no absorption by the neutral hydrogen in the IGM which would reduce the measured fluxes and for GALFORM predictions we assume an escape fraction of $f_{\rm esc} = 0.02$. The predictions from the GALFORM and TM05 models for these future surveys as well as some published surveys are summarised in Table 3.

4.1. DaZle – Dark ages z Lyman-α Explorer

DaZle is a visitor mode instrument placed on the VLT UT3 (Horton et al. 2004). The instrument is designed to use a narrow-band differential imaging technique, i.e. observing the same field with two very narrow filters with slightly offset central wavelength. Objects with Lyα in one of the filters can then be selected from the differential image of both filters. The field-of-view of DaZle is $6.83' \times 6.83'$ and it is expected to reach a flux level of 2×10^{-18} erg s^{-1} cm^{-2} (5σ) in 10 h of integration in one filter. This corresponds to a luminosity limit at redshift $z = 7.7$ of $\log(L_{\rm Ly\alpha}) = 42.13$ erg s^{-1}. The two initial filters are centred on $z_{\rm Ly\alpha} = 7.68$ and 7.73 (with widths $\Delta z = 0.006$ and 0.025 respectively) and at this redshift, the surveyed volume becomes 1340 Mpc^3 per pointing per filter pair. Thus, from Fig. 2, we can conclude that DaZle will discover ∼0.16−0.45 candidates at $z = 7.7$ with one pointing and filter pair.

4.2. ELVIS – Emission Line galaxies with VISTA Survey

ELVIS[1] is part of Ultra-VISTA, a future ESO Public Survey with VISTA[2] (Visible and Infrared Survey Telescope for Astronomy). Ultra-VISTA is planned to do very deep near-infrared broad- and narrow-band imaging in the COSMOS field. It will observe four strips with a total area of 0.9 deg^2. The narrow-band filter is focused on the $z_{\rm Ly\alpha} = 8.8$ sky background window with central wavelength $\lambda_{\rm c} = 1185$ nm, and redshift width $\Delta z = 0.1$. The flux limit of the narrow-band images is expected to reach 3.7×10^{-18} erg s^{-1} cm^{-2} (5σ) after the full survey has been completed. Ultra-VISTA will run from early 2008 for about 5 years and all the data will be public. ELVIS is presented further in Nilsson et al. (2006b). ELVIS will survey several different emission-lines (e.g. Hα at redshift $z = 0.8$, [OIII] at redshift $z = 1.4$ and [OII] at redshift $z = 2.2$) as well as the Lyα line.

When the survey is complete, the final mosaic will reach a Lyα luminosity limit of $\log(L_{\rm Ly\alpha}) = 42.53$ erg s^{-1}. The volume surveyed will be 5.41×10^5 Mpc^3. From Fig. 2 we see that ELVIS should be expected to detect 3−20 LEGOs at $z = 8.8$.

4.3. JWST

A possibility even further into the future is to use the James Webb Space Telescope[3] (JWST). JWST is scheduled for launch

[1] www.astro.ku.dk/~kim/ELVIS.html
[2] www.vista.ac.uk
[3] www.jwst.nasa.gov

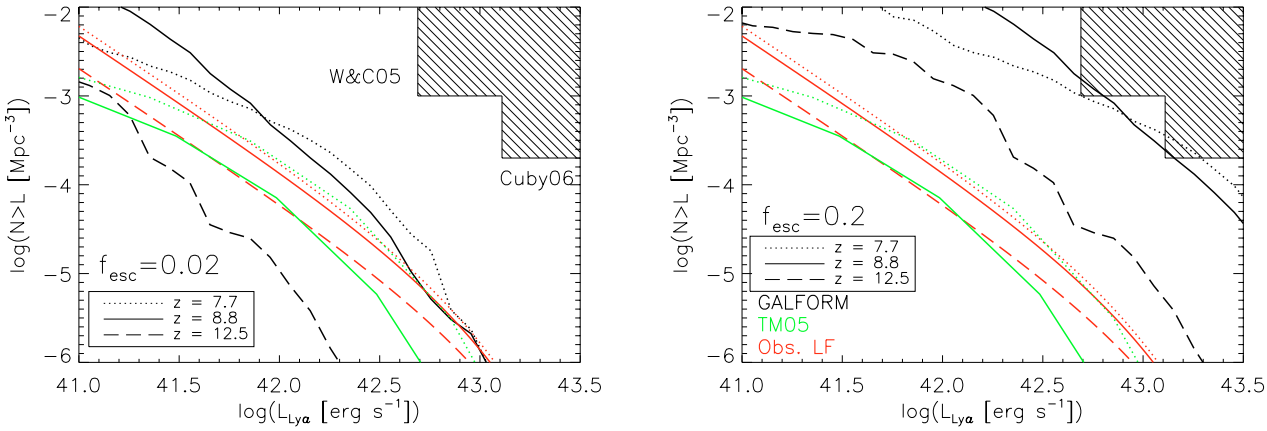

Fig. 2. Predicted Lyα luminosity functions at $z > 7$. Red lines are extrapolations from observed luminosity functions at lower redshift, green lines are TM05 models and black lines are GALFORM models. Different linestyles show different redshifts z = 7.7, 8.8 and 12.5. No prediction is shown for the TM05 model at z = 12.5. Hatched area marks observational upper limits from Willis & Courbin (2005) and Cuby et al. (2006), both at redshift z = 8.8. In the *left panel*, the GALFORM predictions are shown for escape fraction $f_{\rm esc}$ = 0.02 (our standard value), while in the *right panel*, they are shown for $f_{\rm esc}$ = 0.2. The predictions from the other two methods are identical in both panels.

Table 3. Number of predicted/observed objects per observed field in several present and future surveys from two theoretical models. Data from Subaru XMM Deep Field (SXDS) are from Ouchi et al. (2005), Shimasaku et al. (2006) and Kashikawa et al. (2006). GALFORM predictions are made assuming an escape fraction of $f_{\rm esc}$ = 0.02.

Name	Redshift	Area (arcmin^2)	Luminosity limit (5σ, erg s^{-1})	GALFORM	TM05	Observed number
SXDS (Ouchi)	5.7	8100	$10^{42.40}$	443	339	515
SXDS (Shimasaku)	5.7	775	$10^{42.40}$	112	86	83
SXDS (Kashikawa)	6.5	918	$10^{42.27}$	108	57	58
DaZle	7.7	47	$10^{42.13}$	0.45	0.16	–
ELVIS	8.8	3240	$10^{42.50}$	20	2.8	–
Cuby06	8.8	31	$10^{43.10}$	0.0003	0.0	0
W&C05	8.8	6.3	$10^{42.25}$	0.015	0.002	0
JWST	12.5	9.3	$10^{42.00}$	0.018	–	–

in 2013 and will have excellent capabilities within the near- and mid-infrared regions of the spectrum. Two of the instruments aboard JWST could be used for narrow-band surveys; NIRCam, the near-infrared camera, and TFI, the tunable filter imager (for a review on JWST see Gardner et al. 2006). NIRCam will have 31 filters, of which nine are narrow-band filters. The filter with shortest wavelength has central wavelength $\lambda_{\rm c}$ = 1.644 μm (F164N; $z_{{\rm Ly}\alpha}$ = 12.5, Δz = 0.135). TFI will have tunable filters with variable central wavelength, however it is only sensitive at wavelengths larger than $\lambda \sim 1.6$ μm. NIRCam is expected to reach a flux limit of $\sim 1 \times 10^{-18}$ erg s^{-1} cm^{-2} (5σ) in 10 000 s of exposure time. Hence, a flux limit of $\sim 5 \times 10^{-19}$ erg s^{-1} cm^{-2} (5σ, $\log(L_{{\rm Ly}\alpha}(z = 12.5)) = 42.00$ erg s^{-1}) could be reached in 10 h, assuming that the sensitivity is proportional to the square root of the exposure time. TFI is expected to be able to reach a flux limit almost a factor of two deeper in the same time, however it has a field-of-view of only half of the NIRCam (which is $2 \times 2.16' \times 2.16'$). In one NIRCam pointing at redshift z = 12.5, approximately 1640 Mpc^3 are surveyed. Again, from Fig. 2, we can estimate that we will detect $\lesssim$0.1 galaxies per 10-h pointing with NIRCam. However, the number of detections depends strongly on the escape fraction which is unknown at such high redshifts, and thus the number of detected galaxies can be larger.

5. Constraints on the early Universe

Of the surveys at these redshifts that have been presented in previous articles (Horton et al. 2004; Willis & Courbin 2005; Cuby et al. 2006; Nilsson et al. 2006b), or are conceivable (JWST, see Sect. 4.3) only ELVIS will detect a large enough sample to start to measure the luminosity functions and the extent of reionisation at these redshifts and to study the fraction of PopIII stars in the population. We here discuss these issues with respect to ELVIS.

From the semi-analytical modelling, we can make mock observations of the ELVIS survey. The procedure to produce these catalogues is explained in detail in Orsi et al. (in prep.), but the outline of the process is that galaxies from GALFORM are placed in matching dark matter haloes in the Millenium N-body simulation (Springel et al. 2005), which is a cubical volume in a CDM universe of comoving size 500 Mpc/h, thus creating a mock universe with simulated galaxies which includes all the effects of clustering. We can then make mock observations of this simulated Universe, including the same limits on flux, redshift, sky area etc. as for any real survey, and from these observations produce mock galaxy catalogues. From the mock catalogues, we can in turn make mock luminosity functions of Lyα emitters at redshift z = 8.8. In Fig. 3 we plot the "observed" luminosity functions in the 112 mock catalogues taken from different regions of the Millenium simulation volume. Note that for making these mock catalogues, GALFORM was run with the same cosmological parameters as in the Millenium simulation itself, which are slightly different from the "concordance" values assumed elsewhere in this paper, as described in the Introduction (this is why the mean luminosity function for the whole simulation volume which is plotted in Fig. 3 is slightly different from

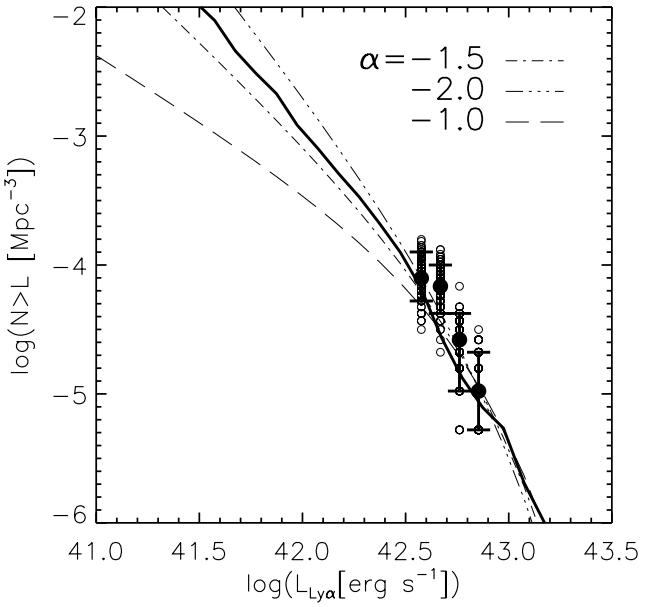

Fig. 3. Luminosity functions at $z = 8.8$ for a set of mock ELVIS surveys computed using GALFORM. The 112 mock surveys are identical apart from being taken from different regions in the Millennium simulation volume. The open circles show number counts in each mock catalogue, in four luminosity bins. The black dot with error bars shows the median of the mocks in each bin, with the error bars showing the 10−90% range. The thin lines are best fit Schechter functions to the median points with different assumed faint end slopes. The thick solid line shows the "true" luminosity function, as measured from model galaxies in the total Millenium simulation volume.

the GALFORM prediction for $z = 8.8$ plotted in Fig. 2). We used escape fraction $f_{\rm esc} = 0.02$. The figure shows that the spread in number density between the different mock catalogues is large, almost a factor of ten in number density in each luminosity bin. This is a consequence both of the small numbers of galaxies in the mock surveys and of galaxy clustering, which causes "cosmic variance" between different sample volumes. The prediction from GALFORM is therefore that it will be difficult to accurately measure the luminosity function of Lyα emitters at $z = 8.8$ even using the sample from the large area ELVIS survey. In particular, there will be no useful constraint on the faint-end slope α. This is simply a consequence of the flux limit of narrow-band surveys, i.e. even if we use the median values of the luminosity function from all the mocks, then Schechter functions with slopes in the range -1 to -2 all give acceptable fits, as illustrated in Fig. 3. However, if all the data are combined in one luminosity bin, it should be possible to measure $\phi^\star$ assuming values for α and $L^\star$. The possibility of including data points from several surveys at different luminosities (e.g. also lensing surveys that probe the faint end of the luminosity function) would also significantly improve the results.

Two suggested methods of constraining reionisation from observations of Lyα emitters, without requiring spectroscopy, are to measure the clustering of Lyα-sources and to compare the Lyα and UV continuum luminosity functions at these redshifts (Kashikawa et al. 2006; Dijkstra et al. 2007a; McQuinn et al. 2007). McQuinn et al. (2007) show that large HII bubbles may exist during reionisation, and that these will enhance the observed clustering of Lyα emitters in proportion to the fraction of neutral hydrogen in the Universe. A sample of ∼50 emitters will be enough to constrain the level of reionisation using this effect (McQuinn, priv. communication), almost within reach of the ELVIS survey. A future, extended version of ELVIS would be able to place very tight constraints on reionisation. In Kashikawa et al. (2006) and Dijkstra et al. (2007a) the use of the combination of the UV and Lyα LFs to constrain the IGM transmission is explored. Lyα emission will be much more susceptible to IGM absorption than the continuum emission and thus the ratio between the two LFs will give information on the level of IGM ionisation. However, with increasing redshift for Lyα, the continuum emission will be increasingly difficult to observe, and it is unclear if this method will be feasible for surveys such as ELVIS.

It is possible that galaxies at $z = 8.8$ still have a significant population of primordial PopIII stars. A test for the fraction of primordial stars is the amount of HeII 1640 Å emission (Schaerer 2003; Tumlinson et al. 2003). Depending on models, these authors predict that the HeII 1640 Å emission line should have a flux between 1−10% of the flux in the Lyα line. For ELVIS $z = 8.8$ Lyα emitters, the HeII 1640 Å line is redshifted to 1.61 μm. Due to the many OH sky emission lines in this region of the spectrum, it would be desirable to try to observe the HeII 1640 Å line from a space-based observatory such as JWST. According to the JWST homepage, NIRSpec will achieve a sensitivity in the medium resolution mode on an emission line at 1.6 μm of $\sim 7 \times 10^{-19}$ erg s^{-1} cm^{-2} (10σ) for an exposure time of 10^5 s (30 h). Thus, if the Lyα emission line has a flux of $\sim 5 \times 10^{-18}$ erg s^{-1} cm^{-2}, the HeII 1640 Å will be marginally detected with JWST in 30 h of integration, depending on the ratio of HeII 1640 Å to Lyα flux. The NIRSpec sensitivity increases at longer wavelengths, but the increasing luminosity distance to galaxy candidates with HeII 1640 Å emission at longer wavelengths will most likely counteract this effect.

6. Discussion

We summarise our predictions for number counts of Lyα emitters in narrow-band surveys in Fig. 4. We also summarise the numbers of detected objects for specific current and future surveys in Table 3. A few comments can be made on the differences in predictions between the two models. Firstly, as can be seen in Fig. 4 and also Fig. 2, the luminosity functions have steeper faint-end slopes in the GALFORM models than in the TM05 models. Secondly, the GALFORM and TM05 models predict similar amounts of evolution at a given flux over the range $z = 6-9$ where they can be compared.

Several factors enter into the error bars of our predictions. One problem is the uncertainties in, and disagreement between, the observed lower redshift luminosity functions which are used to calibrate the theoretical models. There are many caveats in producing Lyα luminosity functions, of which the selection function is the most difficult to correct for. The problem arises from that the filter transmission curve is not box-shaped, but rather gaussian. Thus, only brighter objects will be observed at the wings of the filter, and these will be observed to have smaller than intrinsic luminosities. Secondly, the equivalent width (*EW*) limit that the survey is complete to depends on the depth of the broad-band images used for the selection. Thirdly, if the sample is a photometric sample, it is possible that there are lower redshift interlopers, where the emission line is e.g. [OII], in the sample. Finally, the samples are still so small that we have to deal with small number statistics. All of these problems cause the observed luminosity function at lower redshifts to be uncertain.

Both theoretical models (semi-analytical and phenomenological) have uncertainties resulting from how they model the

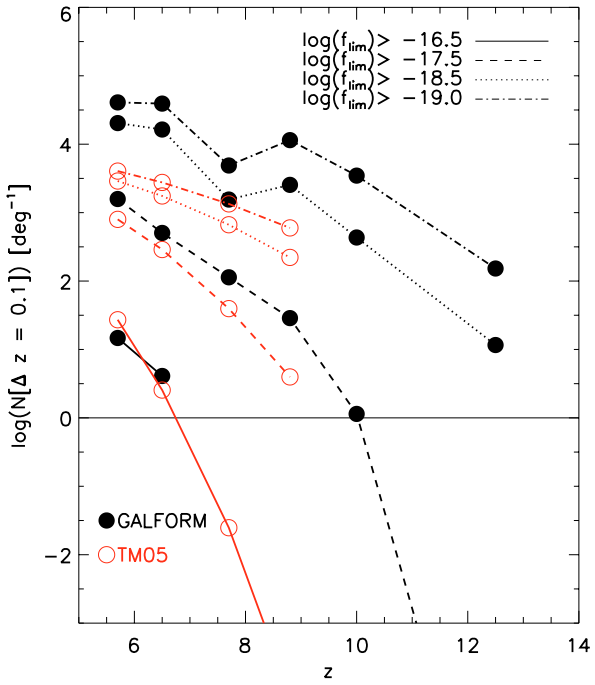

Fig. 4. Summary of predictions. The plot shows the number of Lyα emitting galaxies expected per square degree per redshift interval $\Delta z = 0.1$ as a function of redshift and observed flux limit. The predictions of GALFORM are shown in black and of the TM05 model in red. The different line styles are for different flux limits.

galaxy formation process, and also from the assumption that the fraction of Lyα photons escaping from galaxies is constant and does not change with redshift. In addition, neither model includes attenuation of the Lyα flux due to neutral hydrogen in the IGM. This attenuation would be expected to be strong at $z > z_{\rm reion}$, when the IGM is neutral, and weaker at $z < z_{\rm reion}$, when most of the IGM is ionised. The degree of attenuation depends on a number of different effects, as analysed in Santos (2004), and discussed in Le Delliou et al. (2006), and is currently very uncertain. Nonetheless, this attenuation is expected to produce observable effects on the evolution of the Lyα luminosity function, if reionisation occurs within the redshift range covered by future observations, and so estimating the reionisation redshift and the neutral fraction after reionisation are included in the science goals of these surveys.

It is apparent that the key to acquiring a large sample of Lyα-emitting galaxies at redshifts greater than 7 is both depth and area. In a recent paper, Stark et al. (2007b) suggest that one of the most efficient means of finding very high redshift Lyα emitters is through spectroscopic surveys focused on gravitational lensing clusters. Lensing surveys could easily reach down to a luminosity limit of $10^{40.5}$ erg s^{-1} in a few tens of hours. However, the surveyed volumes are very small, of the order of a hundred Mpc^3. For a lensed survey, the area in the source plane is reduced by the same factor that the flux is amplified, so in principle one gains in the total number of objects detected relative to an unlensed survey if the luminosity function is steeper than $N(>L) \propto L^{-1}$. In the GALFORM and TM05 models, the asymptotic faint-end slope is shallower than this, but at higher luminosities, the slope can be steeper. For example, GALFORM predicts that at $z = 10$, the average slope in the luminosity range 10^{41}–10^{42} erg s^{-1} is close to $N(>L) \propto L^{-2}$ (see Fig. 8 in Le Delliou et al. 2006), so that a lensing amplification of 10 results in 10 times more objects being detected, with intrinsic luminosities 10 times lower, compared to an unlensed survey with the same area and flux limit. Therefore lensing and narrow-band surveys are complementary to each other as they probe different parts of the luminosity function. With either type of survey, reaching a significant sample of redshift $z \sim 7$–8 should be possible in the next few years with telescopes/instruments in use or soon available.

An interesting type of object found recently in narrow-band surveys are the Lyα blobs, large nebulae with diameters up to 150 kpc and Lyα luminosities up to 10^{44} erg s^{-1} with or without counterpart galaxies (e.g. Steidel et al. 2000; Matsuda et al. 2004; Nilsson et al. 2006a). Several mechanisms have been proposed to explain this phenomenon, including starburst galaxies and superwinds, AGN activity or cold accretion. It is interesting to consider if such objects would be detected in any of these surveys, assuming they exist at these redshifts. A typical Lyα blob will have a luminosity of $\sim 10^{43}$ erg s^{-1} and a radius of, say, 25 kpc. This will result in a surface brightness of $\sim 5 \times 10^{39}$ erg s^{-1} kpc^{-2}. Thus, a narrow-band survey will have to reach a flux limit, as measured in a 2″ radius aperture of $\sim 1.3 \times 10^{42}$ erg s^{-1} at redshift $z = 8.8$, corresponding to $\log L = 42.11$. (An aperture radius of around 2″ is expected to be roughly optimal for signal-to-noise.) For lower or higher redshifts, this limit is higher or lower respectively. Thus, ELVIS will not be able to detect Lyα blobs unless they are brighter and/or more compact at higher redshift than a typical blob at lower redshift. DaZle and JWST could in principle detect this type of object, but only if they are very abundant in the very high redshift Universe, due to the small survey volumes of these instruments. It is of course highly uncertain what properties such Lyα blobs would have at $z \sim 7$–9, or their space density, but it appears unlikely that the future surveys presented here would detect any such objects.

To find compact Lyα emitters at redshifts $z \gtrsim 10$ in significant numbers we will probably have to await instruments even further in the future. If a future 40-m ELT (Extremely Large Telescope) was equipped with a wide-field NIR imager and a narrow-band filter of similar width to ELVIS, it could reach a luminosity limit of $L \sim 10^{41.2}$ erg s^{-1} at redshift $z = 10.1$ (where a suitably large atmospheric window exists) in approximately 20 h. Using the GALFORM model for $z = 10$, the number density should be $N(>L) \approx 4 \times 10^{-3}$ Mpc^{-3} at this luminosity limit. Thus, to get a sample of ten Lyα emitters would require imaging an area on the sky of approximately 16 square arcminutes, assuming a narrow-band filter with redshift range $10.05 < z_{\rm Ly\alpha} < 10.15$. This could be achieved with one pointing if the detector has a field-of-view of 6 arcmin on a side, as suggested by the ESO ELT Working Group[4]. It should of course be noted that these are very tentative numbers, but they display the possibilities of far future instruments.

Acknowledgements. The authors wish to thank J. Fynbo, P. Møller, O. Möller, J. Sommer-Larsen and J.-P. Kneib for comments on the manuscript. K.N. gratefully acknowledges support from IDA – Instrumentcenter for Danish Astrophysics. The Dark Cosmology Centre is funded by the DNRF. A.O. acknowledges support of the European Commission's ALFA-II programme through its funding of the Latin-american European Network for Astrophysics and Cosmology (LENAC). C.G.L. is supported by the PPARC rolling grant for extragalactic astronomy and cosmology at Durham. C.M.B. is supported by a Royal Society University Research Fellowship.

References

Ahn, S.-H. 2004, ApJ, 601, L25

[4] http://www.eso.org/projects/e-elt/Publications/ELT_INSWG_FINAL_REPORT.pdf

Ajiki, M., Taniguchi, Y., Fujita, S. S., et al. 2003, AJ, 126, 2091
Barton, E. J., Davé, R., Smith, J.-D. T., et al. 2004, ApJ, 604, L1
Baugh, C. M., Lacey, C. G., Frenk, C. S., et al. 2005, MNRAS, 356, 1191
Cole, S., Lacey, C. G., Baugh, C. M., & Frenk, C. S. 2000, MNRAS, 319, 168
Cuby, J.-G., Hibon, P., Lidman, C., et al. 2007, A&A, 461, 911
Dawson, S., Rhoads, J. E., Malhotra, S., et al. 2007, ApJ, submitted [arXiv:0707.4182]
Le Delliou, M., Lacey, C. G., Baugh, C. M., et al. 2005, MNRAS, 357, L11
Le Delliou, M., Lacey, C. G., Baugh, C. M., & Morris, S. L. 2006, MNRAS, 365, 712
Dijkstra, M., Wyithe, S., & Haiman, Z. 2007a, MNRAS, 379, 253
Dijkstra, M., Lidz, A., & Wyithe, J. S. B. 2007b, MNRAS, 377, 1175
Fardal, M. A., Katz, N., Gardner, J. P., et al. 2001, ApJ, 562, 605
Furlanetto, S. R., Schaye, J., Springel, V., & Hernquist, L. 2005, ApJ, 622, 7
Gardner, J. P., Mather, J. C., Clampin, M., et al. 2006, Space Sci. Rev., 123, 485 [arXiv:astro-ph/0606175]
Gnedin, N. Y., & Prada, F. 2004, ApJ, 608, L77
Gronwall, C., Ciardullo, R., Hickey, T., et al. 2007, ApJ, accepted [arXiv:0705.3917]
Haiman, Z. 2002, ApJ, 576, L1
Haiman, Z., & Spaans, M. 1999, ApJ, 518, 138
Haiman, Z., & Cen, R. 2005, ApJ, 623, 627
Haiman, Z., Spaans, M., & Quataert, E. 2000, ApJ, 537, L5
Horton, A., Parry, I., Bland-Hawthorne, J., et al. 2004 [arXiv:astro-ph/0409080]
Hu, E. M., Cowie, L. L., Capak, P., et al. 2004, ApJ, 127, 563
Iye, M., Ota, K., Kashikawa, N., et al. 2006, Nature, 443, 186
Kashikawa, N., Shimasaku, K., Malkan, M. A., et al. 2006, ApJ, 648, 7
Laursen, P., & Sommer-Larsen, J. 2007, ApJ, 657, L69
Malhotra, S., & Rhoads, J. 2004, ApJ, 617, L5
Malhotra, S., Rhoads, J. E., Pirzkal, N., et al. 2005, ApJ, 626, 666
Matsuda, Y., Yamada, T., Hayashino, T., et al. 2004, AJ, 128, 569
McQuinn, M., Hernquist, L., Zaldarriaga, M., & Dutta, S. 2007, MNRAS, accepted [arXiv:astro-ph/0704.2239]
Miralda-Escudé, J. 1998, ApJ, 501, 15
Miralda-Escudé, J., & Rees, M. J. 1998, ApJ, 497, 21
Møller, P., & Fynbo, J. U. 2001, A&A, 372, L57
Nilsson, K. K., Fynbo, J. P. U., Møller, P., Sommer-Larsen, J., & Ledoux, C. 2006a, A&A, 452, L23
Nilsson, K. K., Fynbo, J. P. U., Møller, P., & Orsi, A. 2006b, to appear in the ASP Conf. Proc. of At the Edge of the Universe, ed. J. Afonso, H. Ferguson, & R. Norris [arXiv:astro-ph/0611239]
Ouchi, M., Shimasaku, K., Akyiama, M., et al. 2005, ApJ, 620, L1
Ouchi, M., Shimasaku, K., Akiyama, M., et al. 2007, ApJ, submitted [arXiv:0707.3161]
Parkes, I. M., Collins, C. A., & Joseph, R. D. 1994, MNRAS, 266, 983
Rousselot, P., Lidman, C., Cuby, J.-G., Moreels, G., & Monnet, G. 2000, A&A, 354, 1134
Santos, M. R. 2004, MNRAS, 349, 1137
Schaerer, D. 2003, A&A, 397, 527
Shimasaku, K., Kashikawa, N., Doi, M., et al. 2006, PASJ, 58, 313
Spergel, D. N., Bean, R., Doré, O., et al. 2007, ApJS, 170, 377
Springel, V., White, S. D. M., Jenkins, A., et al. 2005, Nature, 435, 629
Stark, D. P., Ellis, R. S., Richard, J., et al. 2007a, ApJ, 663, 10
Stark, D. P., Loeb, A., & Ellis, R. S. 2007b, ApJ, submitted [arXiv:astro-ph/0701882]
Steidel, C. C., Adelberger, K. L., Shapley, A. E., et al. 2000, ApJ, 532, 170
Taniguchi, Y., Ajiki, M., Nagao, T., et al. 2005, PASJ, 57, 165
Tapken, C., Appenzeller, I., Gabasch, A., et al. 2006, A&A, 455, 145
Tasitsiomi, A. 2006, ApJ, 645, 792
Thommes, E., & Meisenheimer, K. 2005, A&A, 430, 877
Tumlinson, J., Shull, J. M., & Venkatesan, A. 2003, ApJ, 584, 608
van Breukelen, C., Jarvis, M. J., & Venemans, B. P. 2005, MNRAS, 359, 895
Verhamme, A., Schaerer, D., & Maselli, A. 2006, A&A, 460, 397
Willis, J. P., & Courbin, F. 2005, MNRAS, 357, 1348
Zheng, Z., & Miralda-Escudé, J. 2002, ApJ, 578, 33